



Published in final edited form as:

Brain Behav Immun. 2017 August ; 64: 330–343. doi:10.1016/j.bbi.2017.04.003.

Modulation of experimental arthritis by vagal sensory and central brain stimulation

Gabriel Shimizu Bassi^{a,*}, Daniel Penteado Martins Dias^b, Marcelo Franchin^c, Jimmy Talbot^c, Daniel Gustavo Reis^c, Gustavo Batista Menezes^d, Jaci Airton Castania^b, Norberto Garcia-Cairasco^b, Leonardo Barbosa Moraes Resstel^c, Helio Cesar Salgado^b, Fernando Queiró Cunha^c, Thiago Mattar Cunha^c, Luis Ulloa^{e,*}, and Alexandre Kanashiro^{c,f,*}

^aDepartment of Immunology, Ribeirão Preto Medical School – University of São Paulo, Ribeirão Preto, SP, Brazil

^bDepartment of Physiology, Ribeirão Preto Medical School – University of São Paulo, Ribeirão Preto, SP, Brazil

^cDepartment of Pharmacology, Ribeirão Preto Medical School – University of São Paulo, Ribeirão Preto, SP, Brazil

^dCenter for Gastrointestinal Biology, Department of Morphology, Federal University of Minas Gerais, Belo Horizonte, MG, Brazil

^eDepartment of Surgery, Center of Immunology & Inflammation, Rutgers-New Jersey Medical School, Rutgers University, Newark, NJ 07101, USA

^fDepartment of Physiological Sciences, Federal University of São Carlos, São Carlos, SP, Brazil

Abstract

Articular inflammation is a major clinical burden in multiple inflammatory diseases, especially in rheumatoid arthritis. Biological anti-rheumatic drug therapies are expensive and increase the risk of systemic immunosuppression, infections, and malignancies. Here, we report that vagus nerve stimulation controls arthritic joint inflammation by inducing local regulation of innate immune response. Most of the previous studies of neuromodulation focused on vagal regulation of inflammation via the efferent peripheral pathway toward the viscera. Here, we report that vagal stimulation modulates arthritic joint inflammation through a novel “afferent” pathway mediated by the locus coeruleus (LC) of the central nervous system. Afferent vagal stimulation activates two

*Corresponding authors at: Department of Physiological Sciences, Federal University of São Carlos (UFSCAR), São Carlos, SP, Brazil (A. Kanashiro), shimizug@gmail.com (G.S. Bassi), Luis.Ulloa@Rutgers.edu (L. Ulloa), alex_bioquimica@yahoo.com.br (A. Kanashiro).

Author contributions

G.S.B., L.U., F.Q.C., and A.K. designed the study; G.S.B. and D.P.M. D. performed the surgical procedures and vagus nerve stimulation; G.S.B. and J.T. performed animals experiments; G.S.B. and M.F. performed the ELISA and Western Blotting; D.G.R. and L.R. performed the caudal thermo-analysis, D.P.M.D., J.C. and H.C.S. performed the cardiovascular analysis; G.B.M. and G.S.B. performed the intravital analysis; G.S.B. prepared the figures; G.S.B., L.U., F.Q.C., N.C.G. and A.K. wrote the manuscript; F.Q.C., T.M.C., H.C.S., and A.K. provided financial support.

Disclosures

The authors have no financial conflicts of interest.

Appendix A. Supplementary data

Supplementary data associated with this article can be found, in the online version, at <http://dx.doi.org/10.1016/j.bbi.2017.04.003>.

sympatho-excitatory brain areas: the paraventricular hypothalamic nucleus (PVN) and the LC. The integrity of the LC, but not that of the PVN, is critical for vagal control of arthritic joint inflammation. Afferent vagal stimulation suppresses articular inflammation in the ipsilateral, but not in the contralateral knee to the hemispheric LC lesion. Central stimulation is followed by subsequent activation of joint sympathetic nerve terminals inducing articular norepinephrine release. Selective adrenergic beta-blockers prevent the effects of articular norepinephrine and thereby abrogate vagal control of arthritic joint inflammation. These results reveals a novel neuro-immune brain map with afferent vagal signals controlling side-specific articular inflammation through specific inflammatory-processing brain centers and joint sympathetic innervations.

Keywords

Vagus nerve; Arthritis; Neutrophil migration; Sympathetic nervous system; Neuroimmune interactions; Neuroimmunomodulation

1. Introduction

Articular inflammation is the most typical hallmark and major pathological burden in clinical and experimental arthropathies such as rheumatoid arthritis. Articular inflammation causes joint pain, edema, stiffness as well as loss of functionality due to the infiltration of leukocytes into the synovial cavity and the production of inflammatory cytokines such as tumor necrosis factor (TNF) (Firestein, 2003; Sweeney and Firestein, 2004). Neutrophils are the first type of leukocytes that migrate to the trauma site to eliminate infectious agents and to perform tissue clearance (Firestein, 2003; Sweeney and Firestein, 2004). However, unregulated neutrophilic activity causes joint deformities and motor disabilities as observed in rheumatoid arthritis (Mantovani et al., 2011; Wright et al., 2014). Large amounts of neutrophils are found in the synovial fluid of both clinical and experimental arthritic joint inflammation, especially in the early phases (Firestein, 2003; Kolaczowska and Kubes, 2013; Mohr et al., 1981; Sweeney and Firestein, 2004; Wright et al., 2014). Currently, there is no cure for rheumatoid arthritis and the best available clinical treatments are based on the use of new biological disease-modifying anti-rheumatic drugs (bDMARDs) that act mainly by neutralizing TNF and preventing neutrophil activation (Edrees et al., 2005; Inui and Koike, 2016; Mantovani et al., 2011; Upchurch and Kay, 2012; Wright et al., 2014). These new treatments are still expensive and can increase the risk of infections, malignancies, and immunosuppression (Favalli et al., 2009; Inanc and Direskeneli, 2006; Smitten et al., 2008). Thus, recent experimental efforts focus on the local control of articular inflammation in order to avoid the systemic side-effects of conventional pharmacological therapies. Here, we report that vagal stimulation controls arthritic joint inflammation by inducing a local neuroimmune pathway.

The regulation of immunity by the nervous system has been widely studied, and the discovery of these mechanisms helped to design novel therapeutic strategies for inflammatory diseases (Ordovas-Montanes et al., 2015; Ulloa, 2005). Among these neuroimmune pathways, vagus nerve stimulation (VNS) has received most of the attention due to its potential to control inflammation and improve survival in experimental models of

infectious and inflammatory disorders (Borovikova et al., 2000; Koopman et al., 2016; Levine et al., 2014; Matteoli et al., 2013; Wang et al., 2004). These studies reported that electrical vagal stimulation regulates peripheral inflammation through an efferent peripheral pathway mediated by the sympathetic splenic nerve, splenic lymphocytes producing acetylcholine, and $\alpha 7$ -nicotinic acetylcholine receptors ($\alpha 7$ nAChR) modulating macrophages (Olofsson et al., 2012). However, different investigators have suggested that, in addition to this efferent pathway, vagal stimulation may also trigger afferent signals toward the brain that may contribute to modulate the immune system (Bratton et al., 2012; Cano et al., 2001; Inoue et al., 2016; Martelli et al., 2014; Olofsson et al., 2015; Vida et al., 2011). For example, afferent vagal stimulation decreased bradykinin-induced plasma extravasation by modulating the sympatho-adrenal system (Miao et al., 1997a,b). We also noticed that stimulation of the intact (efferent and afferent) vagus nerve reduced systemic inflammation in $\alpha 7$ nAChR-deficient mice. By contrast, specific efferent stimulation of the distal vagal trunk of the sectioned vagus nerve failed to control systemic inflammation in $\alpha 7$ nAChR-deficient mice (Vida et al., 2011). In addition, VNS protected the kidneys against inflammation-induced injury even when the contralateral vagus nerve was blocked by local anaesthetic inhibiting efferent signals (Inoue et al., 2016). All these studies suggest the existence of an afferent vagal pathway regulating peripheral inflammation via the central nervous system. Here, we report a new central neuroimmune pathway that induces local control of articular inflammation. This novel neuroimmune network reveals specific sympatho-excitatory brain structures regulating local sympathetic components to control arthritic joint inflammation.

2. Material and methods

2.1. Animal experiments

Male Wistar rats (250–300 g), male Swiss and Swiss nude (20–24 g), C57 wild type and C57 TRPV1 KO mice were obtained from the main Animal Facility of the Ribeirão Preto Medical School, University of São Paulo, and housed upon arrival at the animal facility in plastic cages under a 12-h light/dark cycle (lights on at 7am) at $20 \text{ }^{\circ}\text{C} \pm 1 \text{ }^{\circ}\text{C}$. The animals had unrestricted access to food and tap water. The number of animals used was the minimum required to ensure reliability of the results, and every effort was made to minimize animal discomfort. All animals were anesthetized with a mixture of ketamine and xylazine (50 mg/kg and 10 mg/kg, respectively) administered into the right posterior calf muscle through a 30G needle. The experimental protocols comply with the recommendations of the SBNeC (Brazilian Society of Neuroscience and Behavior), the Ethical Principles of the Brazilian College of Animal Experimentation (COBEA Protocols 137/2013, 189/2015) and the US National Institutes of Health Guide for The Care and Use of Laboratory Animals.

2.2. Surgical procedures

After the confirmation of anesthesia by the lack of response to a foot pinch, rats were maintained in supine position, and a medial laparotomy was performed, and one of the following surgical procedures was done: *splenectomy (SPX)*, the spleen was visualized, exposed and then removed after ligation of all splenic blood vessels; *subdiaphragmatic vagotomy (sVNX)*, the posterior wall of the oesophagus was visualized to find the posterior

vagal branch, which was followed until its exit from the oesophageal hiatus, and then 1–2 mm length of the nerve was removed; *sympathectomy (SYMPX)*, the right lumbar sympathetic ganglia (L2–L3 level) were dissected near the renal artery, the L5 ganglion was identified at the level of aorta bifurcation, and all pathways connecting L2 to L5 were excised as we previously described in Bassi et al. (2015); *adrenalectomy (ADX)* was performed after bilateral dorsal incision followed by visualization of the kidneys, both adrenal glands were then removed. Adrenalectomized animals had free access to 0.9% NaCl to avoid body electrolyte loss. *Cervical vagotomy (cVNX)* was performed through a ventral neck approach; the left vagus nerve was dissected from the carotid artery and cut. After each surgery, the wounds were carefully closed with sutures using nylon thread. Experiments were performed 7–10 days after the surgeries.

2.3. Drug administration

All drugs were purchased from Sigma-Aldrich® (Saint Louis, MO, USA) and dissolved in sterile saline solution. The injections were performed in animals under anesthesia and administered through a 30G needle. Different drugs were administered to the animals, alone or in combination, according to the following chronology: (a) Propranolol (5 mg.kg⁻¹/100 µL) was injected into the penile vein 10 min before VNS; (b) Guanethidine (0.3 µg) was injected into the femorotibial joint 48 and 24 h before VNS; (c) Butoxamine (0.3 µg) or atenolol (30 µg) were injected into the femorotibial joint 10 min before VNS; (d) Norepinephrine (NA), procaterol or dobutamine were injected into the femorotibial joint 10 min before the knee zymosan injection; (e) Lidocaine devoid of vasoconstrictors (20 mg.mL⁻¹ – Xylestesin®, Cristália, SP, Brazil) was injected (10 µL) inside the vagus nerve's perineurium just before its entrance under the sternocleidomastoid muscle and 3–5 mm away from the electrodes tip 5 min before vagal stimulation; (f) Cobalt chloride (1 mM CoCl₂ / 0.2 µL), a synaptic transmission blocker (Sandkuhler et al., 1987), was injected 10 min before vagal stimulation into the LC or PVN, through a silica capillary tube (o.d. 150 µm, i.d. 75 µm; Cluzeau Info Lab, France) and infused through an infusion pump (260; Stoelting, Wood Dale, IL, USA) at the rate of 0.1 µL.min⁻¹. The microinjection of cobalt in brain areas has been previously used for functional inactivation (Kretz, 1984) due its property to inhibit synaptic neurotransmission by blocking pre-synaptic calcium channels (Hagiwara and Byerly, 1981). Cobalt blocks only synaptic neurotransmission, while lidocaine blocks both synaptic transmission and the action potential of passage fibers (Sandkuhler et al., 1987). The range of the doses of fMLP, LTB₄ or TNF was selected based on dose-effect curves (Supplementary Fig. 2A,C&E, respectively). All the reagents were dissolved or suspended in sterile saline. Control animals received equal volumes of sterile saline (vehicle) through the same route. A total volume of 50 µL was allowed into the femorotibial joint of rats.

2.4. Zymosan-induced arthritis

Ten or fifty microliters (mice or rats, respectively) of zymosan suspension (30 µg for mice and 100 µg for rats) in sterile saline (0.9 % NaCl; vehicle) were injected into the femorotibial joint (intra-articular; i.a.) of both knees (Gegout et al., 1994; Keystone et al., 1977). *Joint experimental score* was accessed as follows: 0 = no evidence of inflammation; 1 = edema of the femorotibial cavity (slight edema); 2 = edema involving all joint capsule

surrounding the knee (large edema); 3 = the same as 2 plus small hemorrhagic spots along the synovial bursa; 4 = the same as 2 plus large hemorrhagic spots or blood/pus leakage (Bassi et al., 2015). *Joint diameter* was measured by a caliper in millimeters (mm). *Knee neutrophil recruitment*: animals were killed by decapitation and then the knee joint was opened and washed with saline solution containing EDTA (1 mM). Synovial cavities were then opened, washed with a mixture of PBS/EDTA; and the fluid was aspirated with a micropipette, diluted (1:5) and the total number of leukocytes was determined by Neubauer chamber through an optical microscope (400x). The results were depicted as neutrophils/joint cavity.

2.5. Intravital microscopy

In this experiment, mice were used due to experimental limitations regarding knee and microscopy size. One hour after zymosan injection, the animals were anesthetized and the skin surrounding the knee was removed and the patellar tendon was carefully resected to expose the synovial tissue between the femur and tibia. A 20x magnifying objective was used to select 2 to 3 vessels of interest (70–80 μm height) in each mouse knee. After the identification of the synovial blood vessels, rodhamine 6G (Sigma, Saint Louis, MO, USA) was used as a fluorescent marker and was injected intravenously (0.15 mg/kg) immediately before the measurements. The epilluminescence was observed with a 150W variable HBO mercury lamp in conjunction with a Zeiss filter set 15 (546/12-nm band-pass filter, 580-nm Fourier transforms, 590-nm late potentials; Zeiss, Wetzlar, Germany). The images were captured and recorded in a video camera (5100 HS; Panasonic, Secaucus, NJ, USA) and stored in a computer. Data analysis was performed off-line. Rolling leukocytes were considered those cells moving slower than the cells moving through vessel flux, which was measured as the number of cells passing in a fixed point of the vessel per minute. Adherent leukocytes were considered as stationary cells for at least 30 s (1 min recording), and were quantified as the number of cells within a 100 μm length of venule.

2.6. Vagus nerve stimulation in anesthetized animals

Both rats and mice were anesthetized and maintained in supine position. A midline cervical incision was performed, and the right carotid artery was identified. The vagus nerve was then dissected from the right carotid artery and the nerve trunk was placed across a bipolar stainless steel electrode connected to a stimulation device (MP150, Biopac Systems, Santa Barbara, CA, USA). The electrodes were constructed by attaching two 40 mm-long stainless-steel wires (model 791400; 0.005 in. bare, 0.008 in. Teflon coated; A-M Systems, Sequim, WA, USA) to a small plug (GF-6; Microtech, Boothwyn, PA, USA). The bared tips (2 mm-long) of the electrodes were shaped as hooks, with an inter-leads distance of 2 mm. Electrical stimulation was delivered for 2 min and only animals presenting noticeable low breath rate were considered for the experiment (Supplementary Fig. 1C). After the end of the stimulation, the electrode was removed and wounds were closed with sutures. In the sham group, the right vagus nerve was dissected from the carotid artery and a stainless steel electrode was placed across the nerve trunk, but no electrical current was delivered.

2.7. Vagus nerve stimulation and cardiovascular parameters evaluation in unanesthetized rats

Anesthetized rats were maintained in supine position and the right vagus nerve was dissected from the carotid artery through a ventral approach. Briefly, the bared tips of the electrodes (same design employed for the electrical stimulation of anesthetized animals) were implanted around the vagus nerve and exteriorized through the sternocleidomastoid muscle in the nape of the neck. Next, the bipolar stainless steel electrodes were carefully covered with silicone (Kwik-Sil silicone elastomer; World Precision Instruments, Sarasota, FL, USA). Under the same anesthesia, the left carotid artery was catheterized with polyethylene tubing (PE-50; Becton Dickinson, Sparks, MD, USA) for recording the pulsatile arterial pressure (PAP). The catheter was tunneled subcutaneously, exteriorized in the nape of the neck and sutures closed the surgical incision sites. Flunixin meglumine (Banamine, 25 mg/kg, subcutaneous; Schering-Plough, Cotia, SP, Brazil) was injected immediately after the end of surgery. Twenty-four hours after electrode implantation, the arterial catheter was connected to a pressure transducer (MLT844; ADInstruments, Bella Vista, Australia) and the signal was amplified (ML224; ADInstruments, Bella Vista, Australia) and sampled using an IBM/PC computer (Core 2 duo, 2.2 GHz, 4 Gb ram) equipped with an analog-to-digital interface (2 kHz; ML866, ADInstruments, Bella Vista, Australia). A quiet environment was maintained to avoid stress and rats had the PAP recorded at baseline conditions for 15 min. Next, the vagal electrodes were connected to an external electrical stimulator (1M1C; AVS Projetos, São Carlos, SP, Brazil) and rats were subjected to VNS (low intensity VNS: 5 Hz; 0.1 ms; 1 V; or high intensity VNS: 20 Hz; 0.1 ms; 3 V) for 2 min. Rats did not show sign of distress during VNS. A control for proper vagal stimulation is the reduced breath rate during the stimulation. PAP recordings were processed with computer software (LabChart 7.0; ADInstruments, Bella Vista, Australia) capable of detecting inflection points and generate mean arterial pressure (MAP) and heart rate (HR) time series. In the sham group, the electrodes were implanted around the right vagus nerve and exteriorized in the nape of the neck, but no electrical stimulus was delivered.

2.8. Sympathetic chain stimulation in unanesthetized rats

The same electrodes used for the VNS experiment were also used to stimulate the sympathetic chain. Anesthetized animals were subjected to a medial laparotomy under light microscope. The retroperitoneum surrounding the right renal artery was removed for the identification of the L2-L3 fused sympathetic ganglion. Just below the L2-L3 ganglion, bipolar stainless steel electrodes were implanted around the right sympathetic nerve. First, the electrodes were tunneled through the abdominal wall muscles and the small plug was exteriorized in the back of the animal. Next, the short segment bellow L2-L3 of the sympathetic chain implanted with the bipolar stainless steel electrodes was carefully covered with silicone impression material (Kwik-Sil silicone elastomer; World Precision Instruments, Sarasota, FL, USA). The sham group underwent similar surgical procedures but was not subjected to electrical stimulation of the sympathetic chain nerve. Flunixin meglumine (Banamine, 25 mg/kg, subcutaneous; Schering-plough, Cotia, SP, Brazil) was injected immediately after the end of surgery. Twenty-four hours after electrodes implantation, the sympathetic chain was electrically stimulated (0.5 mA; 0.5 ms; 15 Hz) (Hotta et al., 1991) through external stimulation device (1M1C, AVS Projetos, São Carlos,

SP, Brazil). Only those rats that showed no sign of distress during electrical stimulation were used in the study. In the sham group, the electrodes were implanted around the right sympathetic nerve and exteriorized in the nape of the neck, but no electrical stimulus was delivered.

2.9. Temperature measurement in unanesthetized rats

Tail temperature was measured with a thermal camera (Multi-Purpose Thermal Imager IRI 4010; InfraRed Integrated Systems Ltd Park Circle, Tithe Barn Way Swan Valley Northampton, UK), placed 50 cm above the animal's tail, and was plotted as the mean of three measurements recorded at different points throughout the length of the tail. The experiments were conducted in a room kept at 26 ± 1 °C, which is the thermoneutral zone for rats (Gordon, 1990).

2.10. Stereotaxic surgery

Anesthetized Wistar rats were placed in a stereotaxic frame (David Kopf, Tujunga, CA, USA) and underwent the following surgical procedures to introduce stainless steel bipolar electrodes or a guide cannula using coordinates extracted from Rat Brain Atlas (Paxinos and Watson, 2006) with the interaural line serving as the reference for each plane and the upper incisor bar set at 2.5 mm below the interaural line, so that the skull was horizontal between the bregma and lambda. LC: anteroposterior = -1.04 mm, mediolateral = 0.9 mm, dorsoventral = 7.9 mm; PVN: anteroposterior = 7.1 mm, mediolateral = 0.2 mm, dorsoventral = 8.0 mm.

At the end of the surgery, electrodes or guide cannulas were fixed to the skull by acrylic resin and two stainless steel screws; each animal received an intramuscular injection (0.2 mL) of a veterinary antibiotic (Pentabiótico, 0.2 mL; Fort Dodge, Campinas, SP, Brazil), followed by an injection of the anti-inflammatory and analgesic banamine (Flunixin Meglumine, 2.5 mg/kg, Schering-Plough, Cotia, SP, Brazil).

2.11. Brain nuclei stimulation in non-anesthetized rats

Seven to ten days after the stereotaxic surgery, the animals were individually placed in a circular arena (60 cm in diameter and 50 cm high) and the stimulation cable was connected to the bipolar electrodes. A 10 min period of free exploration was allowed. Afterwards, the LC or PVN was electrically stimulated during 2 min by means of a square wave stimulator (1M1C, AVS Projetos, São Carlos, SP, Brazil) according to the following parameters: LC: 20 Hz, 1 ms, 100 μ A (Crawley et al., 1980); PVN: 20 Hz, 0.5 ms, 50 μ A (Kannan et al., 1989). Animals presenting alertness, freezing, escape or seizure behaviors during the stimulation were discarded ($n = 2$). Five minutes after the stimulation the animals were subjected to the Elevated plus-Maze Test. Twenty-four hours after the behavioral experiment, the animals underwent immunological experiments.

2.12. Behavior analysis at the elevated plus-Maze test

To evaluate whether the electrical stimulation procedures produce anxiety-like behaviors, rats were tested in the elevated plusmaze (EPM) 5 min after the end of the stimulation. The elevated plus maze was made of wood and had two open arms (50×10 cm) perpendicular to

two enclosed arms of the same size with 50-cm-high walls, with the exception of the central part (10 × 10 cm), where the arms crossed. The apparatus was elevated 50 cm above the floor (File et al., 2004). The behavior of the animals was analyzed using a video camera positioned 100 cm above the maze. The signal was relayed to a monitor in another room via a closed-circuit television camera to discriminate all forms of behavior. Luminosity at the level of the open arms of the elevated plus maze was 20 lx. A total of 5 min of free exploration of the maze was allowed. The maze was cleaned thoroughly after each test using damp and dry cloths.

2.13. Brain histology

Electrode tips and sites of the microinjections into the LC or PVN were verified histologically. At the end of the experiments, the animals were anesthetized and perfused with 0.1 M phosphate-buffered saline (PBS, pH 7.4) followed by 4% paraformaldehyde and 1 mM potassium ferrocyanide in PBS. A direct current of 1 mA through the tip of the electrodes was then applied for 10 s to permit identification of the stimulation site by Prussian blue reaction. Brains were removed and immersed for 5 h in paraformaldehyde/potassium ferrocyanide solution and then stored for 48 h in 40% sucrose in 0.1 M PBS for cryoprotection. Serial 40 μm brain sections were cut using a cryostat (Leica, Wetzlar, Germany), thaw-mounted on gelatinized slides and stained with hematoxylin-eosin technique in order to localize the sites of microinjection with reference to Paxinos and Watson (2006) Rat Brain Atlas.

2.14. Cytokine and norepinephrine measurement by ELISA

For cytokines assessment the synovial cavities were opened, washed with a mixture of PBS/EDTA (1 mM) by a micropipette and diluted (1:5). The samples were immediately frozen in liquid nitrogen and stored at -70 °C. On the day of the assay, the samples were thawed and maintained in ice until the end of the experiment. The samples were homogenized in 500 μL of the appropriate buffer containing protease inhibitors followed by centrifugation for 10 min at 2000g to collect the supernatant. The supernatant was used to measure the levels of TNF (catalog # DY510), IL-1 β (catalog # DY501), and IL-6 (catalog # DY506) by enzyme-linked immunosorbent assay (ELISA) using Duo set kits from R&D Systems (Minneapolis, MN, USA) according to the user manual. The results were expressed as cytokines concentration in pg·mL⁻¹ based on standard curves.

Knee norepinephrine (NE) level was assessed with articular joint wash with 200 μL of PBS containing sodium metabisulfite (4 mM) and EDTA (1 mM) through a 26G needle and immediately frozen in liquid nitrogen and stored at -70 °C until analysis. After defrosting and centrifugation, the supernatant was used to measure the levels of NE (catalog #KA1891, version 04) by enzyme-linked immunosorbent assay (ELISA) using a set kit from Abnova (Taipei, Taiwan) according to the user manual. The results were expressed as NE concentration in ng·mL⁻¹ based on standard curves.

2.15. Western blot analysis for synovial ICAM-1 measurement

After the completion of the experiment, the animals were decapitated and the synovial tissue surrounding the knee joint was cut and immediately frozen in liquid nitrogen and stored at

–70 °C. On the day of the assay, the samples were immersed in liquid nitrogen, pulverized by a blunt impact, homogenized in a lysis buffer (RIPA buffer, catalog # R0278; Sigma; Saint Louis, MO, USA) containing protease inhibitors (catalog # 5872 s; Cell Signalling, Danvers, MA, USA), and centrifuged for 10 min at 2000g to collect the supernatant. The protein concentration of the lysate was determined by Bradford's assay. The protein samples were separated through an SDS/PAGE gel and transferred to a nitrocellulose membranes (Amersham Pharmacia Biotech, Little Chalfont, UK) followed by overnight incubation at 2–8 °C with primary anti-ICAM1 antibody (1:400) (catalog # WH0003383M1; Sigma, Saint Louis, MO, USA) dissolved in filtered TBS-T buffer containing 5% BSA. On the next day, the membrane was then incubated for 1 h at room temperature with an HRP-conjugated secondary antibody (1:2000; Jackson ImmunoResearch, West Grove, PA, USA). ECL solution (Amersham Pharmacia Biotech, Little Chalfont, UK) was used for the visualization of the membranes' blot in a ChemiDoc MP Imaging System (Bio-Rad Laboratories, Hercules, CA, USA).

2.16. C-Fos immunolabeling

One and half hour after VNS, the animals were anesthetized and perfused with 0.1 M phosphate-buffered saline (PBS, pH 7.4) followed by 4% paraformaldehyde in 0.1 M PBS. Brains and spinal cords were removed and immersed for 5 h in paraformaldehyde and then stored for 72 h in 40% sucrose in 0.1 M PBS for cryoprotection. The brains and spinal cords were sliced (35 μm) in a cryostat (–20 °C) and collected in 0.1 M PBS (pH 7.4) and subsequently processed under free-floating technique according to the avidin–biotin system, using the Vectastain ABC Elite peroxidase rabbit IgG kit (Vector Laboratories, Burlingame, CA, USA). All reactions were performed under agitation at 23 ± 1 °C. The sections were first incubated with 1% H_2O_2 for 10 min and washed three times with 0.1 M PBS (5 min each). Brain and spinal cords sections were then incubated with 0.1 M PBS enriched with 0.1 M glycine, washed three times with 0.1 M PBS (5 min each), and incubated with 0.1 M PBS enriched with 0.2% Triton-X and 1% bovine serum albumin (PBS+) for 1 h. After three washes, the sections were incubated overnight with primary Fos rabbit polyclonal IgG (Santa Cruz Biotechnology, Santa Cruz, CA, USA) at a concentration of 1:1000 (coronal sections) or 1:800 (sagittal sections) in PBS+. Sections were again washed three times (5 min each) with 0.1 M PBS and incubated for 1 h with secondary biotinylated anti-rabbit IgG (H + L; Vectastain, Vector Laboratories, Burlingame, CA, USA) at a concentration of 1:400 in PBS+. After another series of three 5 min washes in 0.1 M PBS, the sections were incubated for 1 h with the avidin–biotin-peroxidase complex (A and B solution of the kit ABC, Vectastain, Vector Laboratories, Burlingame, CA, USA) in 0.1 M PBS at a concentration of 1:200 in 0.1 M PBS and again washed three times in 0.1 M PBS (5 min each). Fos immunoreactivity was revealed by the addition of the chromogen 3,3'-di-aminobenzidine (DAB) (0.02%; Sigma, Saint Louis, MO, USA) to which H_2O_2 (0.04%) was added before use. Finally, tissue sections were washed twice with 0.1 M PBS, mounted on gelatin-coated slides, dehydrated and cover slipped. Fos-positive (Fos+) neurons were visualized under bright-field microscopy as a brown reaction product inside the nuclei. Tissue sections were observed under light microscope (DMI6000b; Leica, Wetzlar, Germany). Darker objects with areas between 10 and 80 μm^2 were identified and automatically counted by a computerized image analysis system (Fiji; www.fiji.sc). Areas

with the same shape and size comprising representative parts of each brain region were used for all rats, and counting of Fos + neurons was performed under a 10× objective. Fos + cells were bilaterally counted in each brain region by a researcher blind to the experimental groups. Nuclei were counted individually and expressed as mean number of Fos + cells per nuclei.

2.17. Statistical analysis

Statistical analyses were performed using Prism 6.0 (GraphPad) software. Neutrophil recruitment to the knee joint, cytokine, behavioral data, and the number of Fos-positive neurons measurement were statistically analyzed by one-way analysis of variance (ANOVA) followed by the Tukey's multiple comparison *post hoc* test. The time course of joint diameter and clinical score were analyzed with the two-way ANOVA for repeated measures followed by the Bonferroni's *post hoc* test when indicated. The hemodynamic parameters were analyzed with the two-way ANOVA for repeated measures followed by the Tukey's *post hoc* test when indicated. The analysis of the difference between two groups was performed with the Student's *t* test. The experimental sample *n* refers to the number of animals and is indicated inside each graph bar and data are expressed as the mean \pm standard error of the mean. Differences were considered statistically significant when $p < 0.05$.

3. Results

3.1. Vagal stimulation attenuated knee joint inflammation via sympathetic neural networks

We first performed right cervical surgical vagotomy in experimental arthritis to analyze whether the vagus nerve regulates joint inflammation. Vagotomy increased neutrophil migration and exacerbated knee joint inflammation in arthritis induced by zymosan (Supplementary Fig. 1A). Conversely, electrical stimulation of the right vagus nerve at low intensity (VNS – 5 Hz, 0.1 ms, 1 V) significantly improved the experimental score of arthritis (Fig. 1A), joint diameter (articular edema) (Fig. 1B), and attenuated neutrophil migration (Fig. 1C) and synovial levels of TNF, IL-1 β , IL-6 and intercellular adhesion molecule (ICAM-1) (Fig. 1D-G). Vagal stimulation also decreased the number of adherent (Fig. 1H) and rolling (Fig. 1I) leukocytes in the synovial microvessels of the knee joint at 1 h after the stimulation (Supplementary Fig. 1B).

Next, we analyzed the relationship between the antiinflammatory effect and the electrical intensity of the vagal stimulation. The anti-inflammatory effect was observed only when the vagus nerve was stimulated at low (VNSL – 5 Hz, 0.1 ms, 1 V), but not at high (VNSH – 20 Hz, 0.1 ms, 3 V) intensity (Fig. 2A). Vagal stimulation at low intensity did not affect heart rate (HR) or mean arterial blood pressure (MAP) (Fig. 2B), but it slightly reduced the breath rate (Supplementary Fig. 1C). Thus, our studies focuses hereafter on the anti-inflammatory mechanism of vagal stimulation at low intensity. Next, we analyzed whether this mechanism was or not specific for the experimental model of arthritis. The anti-inflammatory potential of vagal stimulation is not specific for the experimental model of zymosan-induced arthritis, but it also inhibited inflammation in other experimental models of arthritis and reduced

synovial inflammation induced by other inflammatory stimuli including fMLP (a bacterial chemotactic peptide), LTB₄ (a leukotriene) or direct TNF administration (Supplementary Fig. 2B, D & F).

We analyzed whether vagal stimulation controls arthritic joint inflammation through the mechanisms previously described in experimental sepsis. Vagal stimulation controls peripheral inflammation in sepsis by regulating splenic acetylcholine-producing lymphocytes and dopamine production from adrenal glands (Huston et al., 2006; Peña et al., 2011; Rosas-Ballina et al., 2011; Torres-Rosas et al., 2014). However, vagal regulation of arthritic joint inflammation represents a novel mechanism independent of the spleen, subdiaphragmatic vagus nerve, adrenal glands, lymphocytes or sensory TRPV1 receptors. Vagal stimulation still inhibited arthritic joint inflammation in animals with surgical subdiaphragmatic vagotomy, splenectomy or adrenalectomy (Fig. 2C). These results indicate that this mechanism is independent of the subdiaphragmatic vagus nerve, the spleen and the adrenal glands. Although splenectomy by itself increased knee inflammation, vagal stimulation still reduced synovial neutrophilic infiltration in splenectomized rats (Fig. 2C). Vagal stimulation also inhibited arthritic joint inflammation in lymphocyte-deficient nude mice (Fig. 2D) indicating that this mechanism is independent of lymphocytes. Vagal stimulation also inhibited arthritic joint inflammation in TRPV1-deficient mice (Fig. 2E) indicating that this mechanism is independent of this sensory receptor. Given that the articular joints are richly innervated by sympathetic nerves (Hildebrand et al., 1991; Jimenez-Andrade and Mantyh, 2012; Mach et al., 2002), we analyzed whether they contribute to vagal control of arthritic joint inflammation. Blockade of the sympathetic activity with propranolol, a well characterized adrenergic beta-blocker (McAinsh and Cruickshank, 1990), abolished the vagal regulation of arthritic joint inflammation (Fig. 2F). These results indicate that vagal regulation of arthritic joint inflammation represents a novel anti-inflammatory mechanism as compared to the efferent mechanism of vagal regulation of systemic inflammation in experimental sepsis.

3.2. Central activation is essential to vagal control of arthritic inflammation

Given that the vagal efferent (peripheral) pathways were not required to control arthritic joint inflammation, we speculated about an alternative *afferent* pathway towards the central nervous system. The implication of the central nervous system was assessed by selective vagal afferent stimulation using two approaches to prevent efferent vagal signals: pharmacological efferent inhibition by using intravagal lidocaine, and surgical efferent inhibition by sectioning the distal peripheral vagal nerve. Afferent vagal stimulation induced by either method reduced articular inflammation (Fig. 3A, B). As control, we confirmed that these afferent pathways were not affected by subdiaphragmatic vagotomy, adrenalectomy or splenectomy (Fig. 3C). These results showed that vagal regulation of arthritic joint inflammation is mediated by an afferent vagal pathway toward the central nervous system.

Next, we investigated the brain structures mediating the vagal regulation of arthritic joint inflammation. First, we analyzed what brain structures were activated by vagal afferent stimulation using c-Fos expression, a well-established marker of neuronal activity (Morgan et al., 1987). However, previous studies in the literature of vagal stimulation were performed

in anesthetized animals because anesthesia was required for surgical isolation and electrical stimulation of the vagus nerve. Unfortunately, anesthesia affects both the nervous and the immune systems, and anesthesia itself can affect c-Fos expression. Thus, we developed a novel technical approach of electrical vagal activation in non-anesthetized, awake animals in order to avoid unspecific c-Fos expression. As positive control, we first confirmed that cervical right vagal stimulation induced c-Fos expression in both lateral nucleus of the solitary tract (NTS) and the dorsal motor nucleus (DMN) (Fig. 3D, E, J), central areas previously reported to be activated during vagal stimulation (Cunningham et al., 2008; Naritoku et al., 1995). We observed that vagal stimulation also induced c-Fos expression in the hypothalamic paraventricular nucleus (PVN) and locus coeruleus (LC) (Fig. 3F-J). Thus, we analyzed whether stimulation of these nuclei replicates the vagal control of arthritic joint inflammation. Unilateral electrical stimulation of either the PVN or LC in unanesthetized animals (Supplementary Fig. 3A, B) prevented neutrophil infiltration in both knee joints (Fig. 4A, B). Of note, stimulation of both nuclei did not affect the rat behavior as analyzed by the elevated-plus maze (EPM) test (Supplementary Fig. 3C-H), a well-known model of anxiety (File et al., 2004). On the other hand, the vagal anti-inflammatory effect was abolished by prior unilateral CoCl_2 (a synaptic transmission blocker) microinjection into the LC, but not into the PVN (Fig. 4C, D). Moreover, vagal control of arthritic joint inflammation was inhibited only in the same joint side (ipsilateral) to the hemispheric LC deactivation (Fig. 4C). These results concur with previous studies showing a direct LC innervation to the ipsilateral pre-ganglionic neurons of the spinal cord (Proudfit and Clark, 1991; Westlund et al., 1981). These results indicate that although activation of both nuclei controls arthritic joint inflammation, the integrity of the LC, but not that of the PVN, is required for vagal control of arthritic joint inflammation.

3.3. Vagal stimulation activated local sympathetic control of arthritic joint inflammation

We studied how the sympathetic system mediates the vagal control of arthritic joint inflammation. First, cervical vagal stimulation in unanesthetized rats induced an immediate and transient decrease in the tail skin temperature (Fig. 5A), which mimics the electrical stimulation of the lumbar sympathetic trunk (Fig. 5B). Second, vagal stimulation induced c-Fos expression in both sides of the intermediolateral column of the spinal cord (where sympathetic pre-ganglionic neurons are located) (Fig. 5C). Third, vagal stimulation induced synovial norepinephrine only in the sympathetically innervated ipsilateral knee joint (Fig. 5D). Fourth, the vagal anti-inflammatory signaling was abolished in the knee subjected to either surgical (Fig. 5E) or chemical sympathectomy (Fig. 5F). Fifth, direct electrical stimulation of the lumbar sympathetic trunk mimicked vagal stimulation and reduced neutrophil recruitment in both arthritic knee joints (Fig. 5G). The role of the sympathetic system in modulating arthritic knee inflammation was further confirmed by directly injecting norepinephrine into the joint. Intra-articular injection of norepinephrine decreased joint neutrophil recruitment (Fig. 5H) and synovial ICAM-1 expression (Fig. 5I). We next analyzed the role of the β -adrenergic receptors in the vagal control of arthritic joint inflammation. Intra-articular administration of either atenolol or butoxamine (β_1 - and β_2 -adrenergic blockers, respectively) prevented the vagal regulation of arthritic joint inflammation (Fig. 6A). Conversely, intra-articular injection of either dobutamine or procaterol (β_1 - and β_2 -adrenergic agonists, respectively) mimicked vagal regulation of

arthritic joint inflammation by inhibiting neutrophil migration (Fig. 6B & C, respectively). These results show a novel coordination between the parasympathetic vagus nerve and the sympathetic system to control arthritic joint inflammation.

4. Discussion

Previous studies including multiple experimental models of infectious and inflammatory disorders indicated that the vagus nerve controls peripheral inflammation via *efferent* signals toward the viscera. These mechanisms converge in a “systemic response” based on the release of catecholamines from either the spleen or the adrenal glands to control systemic inflammation (Rosas-Ballina et al., 2008, 2011; Torres-Rosas et al., 2014). Here, we report for the first time vagal regulation of arthritic joint inflammation through an “*afferent*” vagal mechanism mediated by a central locus coeruleus (LC). This anti-inflammatory mechanism is independent of the efferent vagal immunomodulatory components (e.g. spleen, adrenal glands or acetylcholine-producing lymphocytes). In our study, vagal stimulation reduced neutrophil migration and arthritic joint inflammation by activating specific sympatho-excitatory brain nuclei: the LC and PVN. Although direct electrical activation of either nuclei controls arthritic joint inflammation, the integrity of the LC, but not that of PVN, is critical for vagal regulation of arthritic joint inflammation. Unlike efferent vagus nerve, these central nuclei activate specific neuronal networks that induce “local” regulation of inflammation in the arthritic knee joint without inducing a “systemic effect”.

We previously reported a central immune-modulatory arc induced by electrical stimulation of the aortic depressor nerve, an exclusive afferent nerve that can modulate arthritic joint inflammation through the baroreflex activation (Bassi et al., 2015). This similarity with our present study suggests that “peripheral (afferent)-central-peripheral (efferent)” neuronal arcs are important physiological mechanisms modulating the immune system in diverse conditions (Nance et al., 2005) including, acupuncture (Dong et al., 2016; Li et al., 2015), apipuncture (Kwon et al., 2001) and counter-irritation techniques (Bellinger et al., 2013; Miao et al., 1997b,a; Nance et al., 2005; Nance and Sanders, 2007). Our present study dissects this new physiological mechanism showing that cervical vagal stimulation activates the LC and PVN in the central nervous system to induce sympathetic networks modulating arthritic joint inflammation.

Our results indicate that vagal stimulation decreased tail skin temperature due to a sympathetic activation-dependent vasoconstriction of the local vascular bed. Low-intensity vagal stimulation also increased norepinephrine levels in the synovial fluids in control, but not in sympathectomized joints. These results suggest that sympathetic activation is a physiological response to subtle vagal stimulation. These findings concur with previous studies showing spontaneous sympathetic activation after low level vagal stimulation (Ardell et al., 2015; Kember et al., 2014; Onkka et al., 2013). Although the vagus nerve is historically considered the main component of the parasympathetic nervous system, morphological studies demonstrated that this nerve is composed, at the cervical level, by a small population of catecholaminergic fibers (Armour and Randall, 1975, Onkka et al., 2013 Verlinden et al., 2015). Furthermore, different electrical intensities of vagal stimulation can generate opposite effects depending on the “vagal-sympathetic balance”. For instance, low

intensity vagal stimulation induces tachycardia that is slowly reverted as the stimulation intensity increases (Ardell et al., 2015; Kember et al., 2014; Onkka et al., 2013).

Previous immunohistochemical studies showed that antiepileptic vagal stimulation induced c-Fos expression in several brain areas, including the NTS, hypothalamus and LC (Cunningham et al., 2008; Naritoku et al., 1995). In our study, low-intensity vagal stimulation induced c-Fos in the NTS and in specific sympatho-excitatory brain structures such as the LC and PVN. Our results concur with previous studies showing that vagal afferents can regulate LC and PVN (Groves et al., 2005; Olson et al., 1992), and the activation of both nuclei can increase sympathetic activity (Kannan et al., 1989; Samuels and Szabadi, 2008). However, our results show critical new information indicating that electrical stimulation of either the LC or PVN attenuated joint inflammation. Although these results may suggest the involvement of the hypothalamic–pituitary–adrenal (HPA) axis (Silverman and Sternberg, 2012), vagal regulation of arthritic joint inflammation is independent of the adrenal glands and therefore independent of systemic corticosteroids release. Furthermore, although PVN stimulation can influence the activity of other sympathoexcitatory brain areas, as limbic and brainstem structures (Krukoff et al., 2008; Silveira et al., 1995), our results showed that only the integrity of the LC was critical for the VNS effect, as vagal stimulation still controls arthritic joint inflammation in PVN-lesioned animals. In fact, vagal anti-inflammatory potential was suppressed in LC-lesioned animals only in the same side joint to the hemispheric nucleus lesion. These results concur with previous studies showing LC neuronal projections to ipsilateral pre-ganglionic neurons of the spinal cord (Proudfit and Clark, 1991; Westlund et al., 1981).

Our results showed that PVN electrical stimulation reduced knee inflammation, but its integrity is not required for the vagal regulation of arthritic joint inflammation. As PVN receives NTS projections (Cechetto, 2014; Ricardo and Koh, 1978), and it also has direct projections to the LC (Geerling et al., 2010; Holstege, 1987) and the spinal cord (Hosoya et al., 1991; Luiten et al., 1985), we propose that afferent vagal stimulation activates NTS neurons, which in turns synapse with both PVN and LC directly. The NTS-LC information goes to the spinal cord, while the immunomodulatory NTS-PVN network connect to LC neurons and then stimulate spinal cord pre-ganglionic neurons. This hypothesis concurs with previous studies showing that afferent vagal stimulation reduced bradykinin-induced plasma extravasation via an unknown bulbar structure that projects ipsilaterally to sympatho-adrenal preganglionic neurons (Miao et al., 1997b,a). Other studies also suggested the existence of a central sympathomodulatory neuroimmune structure, probably located in the lower brainstem, which is activated after afferent vagal stimulation (Inoue et al., 2016; Vida et al., 2011). In this sense, we propose the LC as the key immunomodulatory mediator between brain and spinal cord, extending our understanding of the central networks controlling peripheral inflammation.

Finally, our results indicate that vagal stimulation attenuated arthritic joint inflammation by increasing norepinephrine levels in the synovial fluid and thereby reducing synovial inflammatory cytokines and ICAM-1. In addition, VNS also attenuated the number of rolling leukocytes in the inflamed synovial microcirculation near to naive levels, showing that vagal stimulation did not induce local vasoconstriction or affected the basal leukocyte

activity. In line with these results, injection of low doses of norepinephrine (1–30 ng) directly into the knee joint reduced local leukocyte infiltration and synovial ICAM-1 expression. These results concur with previous studies suggesting that low levels of norepinephrine can activate β -adrenergic receptors downregulating endothelial ICAM-1 expression (Benschop et al., 1993; Kuroki et al., 2004; OSullivan et al., 2010). On the other hand, the injection of higher norepinephrine concentrations (>100 ng) may progressively activate other synovial receptors (most likely the α -adrenoceptors) that caused a gradual β -adrenergic loss of anti-inflammatory efficacy. We do not rule out that ICAM-1 expression may also be influenced by local physiological changes, as blood flow and shear stress, during the inflammatory response and that norepinephrine can alter the expression of other cell adhesion molecules, as selectins (Niebauer and Cooke, 1996; Rehman et al., 1997). These mechanisms can contribute to the differences observed between neutrophilic infiltration and synovial ICAM-1 expression along the norepinephrine gradient injected into the knee joint.

Articular inflammation is a modern scientific and clinical challenge affecting over 1.5 million of rheumatoid arthritis patients in North America (Myasoedova et al., 2010). Recent clinical and experimental studies showed that vagal stimulation inhibits articular production of TNF, IL-1 β , and IL-6 and improves disease severity in rheumatoid arthritis (Koopman et al., 2016; Levine et al., 2014). In the present study, we show that activation of *afferent* vagal pathways and sympatho-excitatory brain structures control arthritic joint inflammation. Our results suggest that activation of inflammatory processing brain centers by using brain stimulatory methods (such as electrical or magnetic transcranial techniques) could be a potential, low cost and non-invasive therapeutic approach for autoimmune articular diseases. These methods may also provide therapeutic advantages to induce “local” regulation of inflammation and to avoid the “systemic” side-effects of pharmacological anti-TNF therapies (Favalli et al., 2009; Inanc and Direskeneli, 2006; Inui and Koike, 2016).

This study dissects a new neuroimmune pathway induced by afferent vagal signals activating specific inflammatory-processing brain, and thereby specific sympathetic neuronal networks leading to local control of arthritic joint inflammation (Fig. 7). Our data support two current brain theories: the existence of the *immunological homunculus* with a direct role in brain-immune responses (Cohen and Young, 1991; Tracey, 2007); and the *polyvagal theory* where different vagal subsystems are critical to control behavior and emotions (Porges, 2011). We do not rule out the possibility that both systems could act in synchrony to influence immune response-directed behaviors (Bassi et al., 2012; Filiano et al., 2016).

In conclusion, although previous studies have extensively examined the role of sympathetic innervations in arthritis (Bellinger et al., 2013; Janig, 2014; Schaible and Straub, 2014), our results provide a novel neural network coordinating vagal signals with sympathetic-structures via the LC. This new physiological mechanism allows the design of novel therapeutic strategies that may provide clinical advantages as compared to current pharmacological strategies. Since central immunomodulatory information flows through established brain network, our results depict an integrated neuroimmune brain map to control arthritic joint inflammation avoiding the clinical limitations of pharmacological or surgical (invasive) treatments.

Supplementary Material

Refer to Web version on PubMed Central for supplementary material.

Acknowledgments

This study was supported by São Paulo Research Foundation (FAPESP – Brazil) grants: 2011/20343-4, 2012/04237-2, 2013/08216-2, 2013/20549-7, and 2015/20463-0). GSB holds a PhD scholarship from National Council of Technological and Scientific Development (CNPq – Brazil) (proc. N° 142068/2012-8).

References

- Ardell JL, Rajendran PS, Nier HA, KenKnight BH, Armour JA, 2015 Central-peripheral neural network interactions evoked by vagus nerve stimulation: functional consequences on control of cardiac function. *Am. J. Physiol. Heart Circ. Physiol* 309, 1740–1752.
- Armour JA, Randall WC, 1975 Functional anatomy of canine cardiac nerves. *Acta Anat. (Basel)* 91, 510–528. [PubMed: 1171567]
- Bassi GS, Kanashiro A, Santin FM, de Souza GE, Nobre MJ, Coimbra NC, 2012 Lipopolysaccharide-induced sickness behaviour evaluated in different models of anxiety and innate fear in rats. *Basic Clin. Pharmacol. Toxicol* 110, 359–369. 10.1111/j.1742-7843.2011.00824.x. [PubMed: 22059515]
- Bassi GS, Brognara F, Castania JA, Talbot J, Cunha TM, Cunha FQ, Ulloa L, Kanashiro A, Dias DP, Salgado HC, 2015 Baroreflex activation in conscious rats modulates the joint inflammatory response via sympathetic function. *Brain Behav. Immun* 49, 140–147. 10.1016/j.bbi.2015.05.002. [PubMed: 25986215]
- Bellinger DL, Nance DM, Lorton D, 2013 Innervation of the Immune System In: *The Wiley-Blackwell Handbook of Psychoneuroimmunology*. Wiley-Blackwell, pp. 24–72.
- Benschop RJ, Oostveen FG, Heijnen CJ, Ballieux RE, 1993 Beta 2-adrenergic stimulation causes detachment of natural killer cells from cultured endothelium. *Eur. J. Immunol* 23, 3242–3247. 10.1002/eji.1830231230. [PubMed: 8258340]
- Borovikova LV, Ivanova S, Zhang M, Yang H, Botchkina GI, Watkins LR, Wang H, Abumrad N, Eaton JW, Tracey KJ, 2000 Vagus nerve stimulation attenuates the systemic inflammatory response to endotoxin. *Nature* 405, 458–462. 10.1038/35013070. [PubMed: 10839541]
- Bratton BO, Martelli D, McKinley MJ, Trevaks D, Anderson CR, McAllen RM, 2012 Neural regulation of inflammation: no neural connection from the vagus to splenic sympathetic neurons. *Exp. Physiol* 97, 1180–1185. 10.1113/expphysiol.2011.061531. [PubMed: 22247284]
- Cano G, Sved AF, Rinaman L, Rabin BS, Card JP, 2001 Characterization of the central nervous system innervation of the rat spleen using viral transneuronal tracing. *J. Comp. Neurol* 439, 1–18. 10.1002/cne.1331. [PubMed: 11579378]
- Cechetto DF, 2014 Cortical control of the autonomic nervous system. *Exp. Physiol* 99, 326–331. 10.1113/expphysiol.2013.075192. [PubMed: 24121283]
- Cohen IR, Young DB, 1991 Autoimmunity, microbial immunity and the immunological homunculus. *Immunol. Today* 12, 105–110. 10.1016/0167-5699(91)90093-9. [PubMed: 2059311]
- Crawley JN, Maas JW, Roth RH, 1980 Evidence against specificity of electrical stimulation of the nucleus locus coeruleus in activating the sympathetic nervous system in the rat. *Brain Res.* 183, 301–311. [PubMed: 7353141]
- Cunningham JT, Mifflin SW, Gould GG, Frazer A, 2008 Induction of c-Fos and DeltaFosB immunoreactivity in rat brain by Vagal nerve stimulation. *Neuropsychopharmacology* 33, 1884–1895. 10.1038/sj.npp.1301570. [PubMed: 17957222]
- Dong Z-Q, Zhu J, Lu D, Chen Q, Xu Y, 2016 Effect of Electroacupuncture in “Zusanli” and “Kunlun” Acupoints on TLR4 Signaling Pathway of Adjuvant Arthritis Rats. *Am. J. Ther.* 1 10.1097/mjt.0000000000000477.
- Edrees AF, Misra SN, Abdou NI, 2005 Anti-tumor necrosis factor (TNF) therapy in rheumatoid arthritis: correlation of TNF-alpha serum level with clinical response and benefit from changing

- dose or frequency of infliximab infusions. *Clin. Exp. Rheumatol* 23, 469–474. [PubMed: 16095114]
- Favalli EG, Desiati F, Atzeni F, Sarzi-Puttini P, Caporali R, Pallavicini FB, Gorla R, Filippini M, Marchesoni A, 2009 Serious infections during anti-TNF treatment in rheumatoid arthritis patients. *Autoimmun. Rev* 8, 266–273. 10.1016/j.autrev.2008.11.002. [PubMed: 19022409]
- File SE, Lippa AS, Beer B, Lippa MT, 2004 Animal tests of anxiety. *Curr. Protoc. Neurosci* 10.1002/0471142301.ns0803s26. Chapter 8.
- Filiano AJ, Xu Y, Tustison NJ, Marsh RL, Baker W, Smirnov I, Overall CC, Gadani SP, Turner SD, Weng Z, Peerzade SN, Chen H, Lee KS, Scott MM, Beenhakker MP, Litvak V, Kipnis J, 2016 Unexpected role of interferon- in regulating neuronal connectivity and social behaviour. *Nature* 535, 425–429. 10.1038/nature18626. [PubMed: 27409813]
- Firestein GS, 2003 Evolving concepts of rheumatoid arthritis. *Nature* 423, 356–361. 10.1038/nature01661. [PubMed: 12748655]
- Geerling JC, Shin J-W, Chimenti PC, Loewy AD, 2010 Paraventricular hypothalamic nucleus: Axonal projections to the brainstem. *J. Comp. Neurol* 518, 1460–1499. 10.1002/cne.22283. [PubMed: 20187136]
- Gegout P, Gillet P, Chevrier D, Guingamp C, Terlain B, Netter P, 1994 Characterization of zymosan-induced arthritis in the rat: effects on joint inflammation and cartilage metabolism. *Life Sci.* 55, PL321–PL326. 10.1016/0024-3205(94)00771-3. [PubMed: 7934634]
- Gordon CJ, 1990 Thermal biology of the laboratory rat. *Physiol. Behav* 47, 963–991. 10.1016/0031-9384(90)90025-y. [PubMed: 2201986]
- Groves DA, Bowman EM, Brown VJ, 2005 Recordings from the rat locus coeruleus during acute vagal nerve stimulation in the anaesthetised rat. *Neurosci. Lett* 379, 174–179. 10.1016/j.neulet.2004.12.055. [PubMed: 15843058]
- Hagiwara S, Byerly L, 1981 Calcium channel. *Ann. Rev. Neurosci* 4, 69–125. 10.1146/annurev.ne.04.030181.000441. [PubMed: 6261668]
- Hildebrand C, Öqvist G, Brax L, Tuisku F, 1991 Anatomy of the rat knee joint and fibre composition of a major articular nerve. *Anat. Rec* 229, 545–555. 10.1002/ar.1092290415. [PubMed: 2048758]
- Holstege G, 1987 Some anatomical observations on the projections from the hypothalamus to brainstem and spinal cord: an HRP and autoradiographic tracing study in the cat. *J. Comp. Neurol* 260, 98–126. 10.1002/cne.902600109. [PubMed: 3496365]
- Hosoya Y, Sugiura Y, Okado N, Loewy AD, Kohno K, 1991 Descending input from the hypothalamic paraventricular nucleus to sympathetic preganglionic neurons in the rat. *Exp. Brain Res* 85, 10–20. [PubMed: 1884750]
- Hotta H, Nishijo K, Sato A, Sato Y, Tanzawa S, 1991 Stimulation of lumbar sympathetic trunk produces vasoconstriction of the vasa nervorum in the sciatic nerve via α -adrenergic receptors in rats. *Neurosci. Lett* 133, 249–252. 10.1016/0304-3940(91)90581-d. [PubMed: 1667816]
- Huston JM, Ochani M, Rosas-Ballina M, Liao H, Ochani K, Pavlov VA, Gallowitsch-Puerta M, Ashok M, Czura CJ, Foxwell B, Tracey KJ, Ulloa L, 2006 Splenectomy inactivates the cholinergic antiinflammatory pathway during lethal endotoxemia and polymicrobial sepsis. *J. Exp. Med* 203, 1623–1628. 10.1084/jem.20052362. [PubMed: 16785311]
- Inanc N, Direskeneli H, 2006 Serious infections under treatment with TNF-antagonists compared to traditional DMARDs in patients with rheumatoid arthritis. *Rheumatol. Int* 27, 67–71. 10.1007/s00296-006-0165-9. [PubMed: 16896990]
- Inoue T, Abe C, Sung SJ, Moscalu S, Jankowski J, Huang L, Ye H, Rosin DL, Guyenet PG, Okusa MD, 2016 Vagus nerve stimulation mediates protection from kidney ischemia-reperfusion injury through 7nAChR+. splenocytes. *J. Clin. Invest* 126, 1939–1952. 10.1172/jci83658. [PubMed: 27088805]
- Inui K, Koike T, 2016 Combination therapy with biologic agents in rheumatic diseases: current and future prospects. *Ther. Adv. Musculoskeletal Dis* 8, 192–202. 10.1177/1759720x16665330.
- Janig W, 2014 Sympathetic nervous system and inflammation: a conceptual view. *Auton. Neurosci* 182, 4–14. 10.1016/j.autneu.2014.01.004. [PubMed: 24525016]

- Jimenez-Andrade JM, Mantyh PW, 2012 Sensory and sympathetic nerve fibers undergo sprouting and neuroma formation in the painful arthritic joint of geriatric mice. *Arthritis Res. Ther* 14, R101 10.1186/ar3826. [PubMed: 22548760]
- Kannan H, Hayashida Y, Yamashita H, 1989 Increase in sympathetic outflow by paraventricular nucleus stimulation in awake rats. *Am. J. Physiol* 256, 1325–1330.
- Kember G, Ardell JL, Armour JA, Zamir M, 2014 Vagal nerve stimulation therapy: what is being stimulated? *PLoS ONE* 9, e114498 10.1371/journal.pone.0114498. [PubMed: 25479368]
- Keystone EC, Schorlemmer HU, Pope C, Allison AC, 1977 Zymosan—induced arthritis. *Arthritis Rheum.* 20, 1396–1401.10.1002/art.1780200714. [PubMed: 911357]
- Kolaczowska E, Kubes P, 2013 Neutrophil recruitment and function in health and inflammation. *Nat. Rev. Immunol* 13, 159–175. 10.1038/nri3399. [PubMed: 23435331]
- Koopman FA, Chavan SS, Miljko S, Grazio S, Sokolovic S, Schuurman PR, Mehta AD, Levine YA, Faltys M, Zitnik R, Tracey KJ, Tak PP, 2016 Vagus nerve stimulation inhibits cytokine production and attenuates disease severity in rheumatoid arthritis. *Proc. Natl. Acad. Sci* 113, 8284–8289. 10.1073/pnas.1605635113. [PubMed: 27382171]
- Kretz R, 1984 Local cobalt injection: a method to discriminate presynaptic axonal from postsynaptic neuronal activity. *J. Neurosci. Methods* 11 (2), 129–135. [PubMed: 6090819]
- Krukoff TL, Harris KH, Linetsky E, Jhamandas JH, 2008 Expression of c-fos protein in rat brain elicited by electrical and chemical stimulation of the hypothalamic paraventricular nucleus. *Neuroendocrinology* 59, 590–602. 10.1159/000126709.
- Kuroki K, Takahashi HK, Iwagaki H, Murakami T, Kuinose M, Hamanaka S, Minami K, Nishibori M, Tanaka N, Tanemoto K, 2004 Beta2-adrenergic receptor stimulation-induced immunosuppressive effects possibly through down-regulation of co-stimulatory molecules, ICAM-1, CD40 and CD14 on monocytes. *J. Int. Med. Res* 32, 465–483. [PubMed: 15458278]
- Kwon Y, Lee J, Lee H, Han H, Mar W, Kang S, Beitz AJ, Lee J, 2001 Bee venom injection into an acupuncture point reduces arthritis associated edema and nociceptive responses. *Pain* 90, 271–280. 10.1016/s0304-3959(00)00412-7. [PubMed: 11207399]
- Levine YA, Koopman FA, Faltys M, Caravaca A, Bendele A, Zitnik R, Vervoordeldonk MJ, Tak PP, 2014 Neurostimulation of the cholinergic anti-inflammatory pathway ameliorates disease in rat collagen-induced arthritis. *PLoS ONE* 9, e104530 10.1371/journal.pone.0104530. [PubMed: 25110981]
- Li J, Li J, Chen R, Cai G, 2015 Targeting NF- κ B and TNF- α activation by electroacupuncture to suppress collagen-induced rheumatoid arthritis in model rats. *Altern. Ther. Health Med* 21, 26–34.
- Luiten PGM, ter Horst GJ, Karst H, Steffens AB, 1985 The course of paraventricular hypothalamic efferents to autonomic structures in medulla and spinal cord. *Brain Res.* 329, 374–378. 10.1016/0006-8993(85)90554-2. [PubMed: 3978460]
- Mach D, Rogers S, Sabino M, Luger N, Schwei M, Pomonis J, Keyser C, Clohisy D, Adams D, O’Leary P, Mantyh P, 2002 Origins of skeletal pain: sensory and sympathetic innervation of the mouse femur. *Neuroscience* 113, 155–166. 10.1016/s0306-4522(02)00165-3. [PubMed: 12123694]
- Mantovani A, Cassatella MA, Costantini C, Jaillon S, 2011 Neutrophils in the activation and regulation of innate and adaptive immunity. *Nat. Rev. Immunol* 11, 519–531. 10.1038/nri3024. [PubMed: 21785456]
- Martelli D, Yao ST, Mancera J, McKinley MJ, McAllen RM, 2014 Reflex control of inflammation by the splanchnic anti-inflammatory pathway is sustained and independent of anesthesia. *Am. J. Physiol. Regul. Integr. Comp. Physiol* 307, 1085–1091. 10.1152/ajpregu.00259.2014.
- Matteoli G, Gomez-Pinilla PJ, Nemethova A, Giovangiulio MD, Cailotto C, van Bree SH, Michel K, Tracey KJ, Schemann M, Boesmans W, Berghe PV, Boeckxstaens GE, 2013 A distinct vagal anti-inflammatory pathway modulates intestinal muscularis resident macrophages independent of the spleen. *Gut* 63, 938–948. 10.1136/gutjnl-2013-304676. [PubMed: 23929694]
- McAinsh J, Cruickshank JM, 1990 Beta-blockers and central nervous system side effects. *Pharmacol. Ther* 46, 163–197. 10.1016/0163-7258(90)90092-g. [PubMed: 1969642]

- Miao FJ, Jänig W, Green PG, Levine JD, 1997a Inhibition of bradykinin-induced plasma extravasation produced by noxious cutaneous and visceral stimuli and its modulation by vagal activity. *J. Neurophysiol* 78, 1285–1292. [PubMed: 9310420]
- Miao FJ, Jänig W, Levine JD, 1997b Vagal branches involved in inhibition of bradykinin-induced synovial plasma extravasation by intrathecal nicotine and noxious stimulation in the rat. *J. Physiol* 498, 473–481. 10.1113/jphysiol.1997.sp021873. [PubMed: 9032694]
- Mohr W, Wild A, Wolf HP, 1981 Role of polymorphs in inflammatory cartilage destruction in adjuvant arthritis of rats. *Ann. Rheum. Dis* 40, 171–176. [PubMed: 7224688]
- Morgan J, Cohen D, Hempstead J, Curran T, 1987 Mapping patterns of c-fos expression in the central nervous system after seizure. *Science* 237, 192–197. 10.1126/science.3037702. [PubMed: 3037702]
- Myasoedova E, Crowson CS, Kremers HM, Therneau TM, Gabriel SE, 2010 Is the incidence of rheumatoid arthritis rising?: Results from Olmsted County, Minnesota, 1955–2007. *Arthritis Rheum.* 62, 1576–1582. 10.1002/art.27425. [PubMed: 20191579]
- Nance DM, Sanders VM, 2007 Autonomic innervation and regulation of the immune system (1987–2007). *Brain Behav. Immun* 21, 736–745. 10.1016/j.bbi.2007.03.008. [PubMed: 17467231]
- Nance DM, Luczy-Bachman G, Min P, Lee Y-B, Cho Z-H, 2005 The immunomodulatory effects of counter-irritation are mediated via the sympathetic nervous system. *Brain Behav. Immun* 19, e52–e53. 10.1016/j.bbi.2005.10.108.
- Naritoku DK, Terry WJ, Helfert RH, 1995 Regional induction of fos immunoreactivity in the brain by anticonvulsant stimulation of the vagus nerve. *Epilepsy Res.* 22, 53–62. [PubMed: 8565967]
- Niebauer J, Cooke JP, 1996 Cardiovascular effects of exercise: role of endothelial shear stress. *J. Am. Coll. Cardiol* 28, 1652–1660. 10.1016/s0735-1097(96)00393-2. [PubMed: 8962548]
- Olofsson PS, Levine YA, Caravaca A, Chavan SS, Pavlov VA, Faltys M, Tracey Kevin J., 2015 Single-pulse and unidirectional electrical activation of the cervical vagus nerve reduces tumor necrosis factor in endotoxemia. *Bioelectron. Med* 2, 37–42. 10.15424/bioelectronmed.2015.00006.
- Olofsson PS, Rosas-Ballina M, Levine YA, Tracey KJ, 2012 Rethinking inflammation: neural circuits in the regulation of immunity. *Immunol. Rev* 248 (1), 188–204. 10.1111/j.1600-065X.2012.01138.x. [PubMed: 22725962]
- Olson BR, Hoffman GE, Sved AF, Stricker EM, Verbalis JG, 1992 Cholecystokinin induces c-fos expression in hypothalamic oxytocinergic neurons projecting to the dorsal vagal complex. *Brain Res.* 569, 238–248. 10.1016/0006-8993(92)90635-m. [PubMed: 1371708]
- Onkka P, Maskoun W, Rhee KS, Hellyer J, Patel J, Tan J, Chen LS, Vinters HV, Fishbein MC, Chen PS, 2013 Sympathetic nerve fibers and ganglia in canine cervical vagus nerves: localization and quantitation. *Heart Rhythm.* 10, 585–591. 10.1016/j.hrthm.2012.12.015. [PubMed: 23246597]
- Ordovas-Montanes J, Rakoff-Nahoum S, Huang S, Riolo-Blanco L, Barreiro O, von Andrian UH, 2015 The regulation of immunological processes by peripheral neurons in homeostasis and disease. *Trends Immunol.* 36, 578–604. 10.1016/j.it.2015.08.007. [PubMed: 26431937]
- OSullivan JB, Ryan KM, Harkin A, Connor TJ, 2010 Noradrenaline reuptake inhibitors inhibit expression of chemokines IP-10 and RANTES and cell adhesion molecules VCAM-1 and ICAM-1 in the CNS following a systemic inflammatory challenge. *J. Neuroimmunol* 220, 34–42. 10.1016/j.jneuroim.2009.12.007. [PubMed: 20061033]
- Paxinos G, Watson C, 2006 *The Rat Brain in Stereotaxic Coordinates: Hard Cover Edition.* Elsevier Science.
- Peña G, Cai B, Ramos L, Vida G, Deitch EA, Ulloa L, 2011 Cholinergic regulatory lymphocytes re-establish neuromodulation of innate immune responses in sepsis. *J. Immunol* 187, 718–725. 10.4049/jimmunol.1100013. [PubMed: 21666060]
- Porges S, 2011 *The Polyvagal Theory : Neurophysiological Foundations of Emotions, Attachment, Communication, and Self-regulation.* W.W. Norton, New York.
- Proudfit HK, Clark FM, 1991 The projections of locus coeruleus neurons to the spinal cord. *Prog. Brain Res* 88, 123–141. [PubMed: 1813919]
- Rehman J, Mills PJ, Carter SM, Chou J, Thomas J, Maisel AS, 1997 Dynamic exercise leads to an increase in circulating ICAM-1: further evidence for adrenergic modulation of cell adhesion. *Brain Behav. Immun* 11, 343–351. 10.1006/brbi.1997.0498. [PubMed: 9512820]

- Ricardo JA, Koh ET, 1978 Anatomical evidence of direct projections from the nucleus of the solitary tract to the hypothalamus, amygdala, and other forebrain structures in the rat. *Brain Res.* 153, 1–26. [PubMed: 679038]
- Rosas-Ballina M, Ochani M, Parrish WR, Ochani K, Harris YT, Huston JM, Chavan S, Tracey KJ, 2008 Splenic nerve is required for cholinergic antiinflammatory pathway control of TNF in endotoxemia. *Proc. Natl. Acad. Sci. U.S.A* 105, 11008–11013. 10.1073/pnas.0803237105. [PubMed: 18669662]
- Rosas-Ballina M, Olofsson PS, Ochani M, Valdes-Ferrer SI, Levine YA, Reardon C, Tusche MW, Pavlov VA, Andersson U, Chavan S, Mak TW, Tracey KJ, 2011 Acetylcholine-synthesizing T cells relay neural signals in a vagus nerve circuit. *Science* 334, 98–101. 10.1126/science.1209985. [PubMed: 21921156]
- Samuels E, Szabadi E, 2008 Functional neuroanatomy of the noradrenergic locus coeruleus: its roles in the regulation of arousal and autonomic function part I: principles of functional organisation. *Curr. Neuropharmacol* 6, 235–253. 10.2174/157015908785777229. [PubMed: 19506723]
- Sandkuhler J, Maisch B, Zimmermann M, 1987 The use of local anaesthetic microinjections to identify central pathways: a quantitative evaluation of the time course and extent of the neuronal block. *Exp. Brain Res* 68 10.1007/bf00255242.
- Schaible HG, Straub RH, 2014 Function of the sympathetic supply in acute and chronic experimental joint inflammation. *Auton. Neurosci* 182, 55–64. [PubMed: 24423405]
- Silveira MCL, Sandner G, Scala GD, Graeff FG, 1995 C-fos immunoreactivity in the brain following electrical or chemical stimulation of the medial hypothalamus of freely moving rats. *Brain Res.* 674, 265–274. 10.1016/0006-8993(94)01451-m. [PubMed: 7796106]
- Silverman MN, Sternberg EM, 2012 Glucocorticoid regulation of inflammation and its functional correlates: from HPA axis to glucocorticoid receptor dysfunction. *Ann. N. Y. Acad. Sci* 1261, 55–63. 10.1111/j.1749-6632.2012.06633.x. [PubMed: 22823394]
- Smitten AL, Simon TA, Hochberg MC, Suissa S, 2008 A meta-analysis of the incidence of malignancy in adult patients with rheumatoid arthritis. *Arthritis Res. Ther* 10, R45 10.1186/ar2404. [PubMed: 18433475]
- Sweeney SE, Firestein GS, 2004 Rheumatoid arthritis: regulation of synovial inflammation. *Int. j. Biochem. Cell Biol* 36, 372–378. 10.1016/s1357-2725(03)00259-0. [PubMed: 14687914]
- Torres-Rosas R, Yehia G, Peña G, Mishra P, del Rocio Thompson-Bonilla M, Moreno-Eutimio MA, Arriaga-Pizano LA, Isibasi A, Ulloa L, 2014 Dopamine mediates vagal modulation of the immune system by electroacupuncture. *Nat. Med* 20, 291–295. 10.1038/nm.3479. [PubMed: 24562381]
- Tracey KJ, 2007 Physiology and immunology of the cholinergic antiinflammatory pathway. *J. Clin. Invest.* 117, 289–296. 10.1172/jci30555. [PubMed: 17273548]
- Ulloa L, 2005 The vagus nerve and the nicotinic anti-inflammatory pathway. *Nat. Rev. Drug Discovery* 4, 673–684. 10.1038/nrd1797. [PubMed: 16056392]
- Upchurch KS, Kay J, 2012 Evolution of treatment for rheumatoid arthritis. *Rheumatology* 51, vi28–vi36. 10.1093/rheumatology/kes278. [PubMed: 23221584]
- Verlinden TJ, Rijkers K, Hoogland G, Herrler A, 2015 Morphology of the human cervical vagus nerve: implications for vagus nerve stimulation treatment. *Acta Neurol. Scand* 10.1111/ane.12462.
- Vida G, Peña G, Deitch EA, Ulloa L, 2011 A7-cholinergic receptor mediates vagal induction of splenic norepinephrine. *J. Immunol* 186, 4340–4346 10.4049/jimmunol.1003722. [PubMed: 21339364]
- Wang H, Liao H, Ochani M, Justiniani M, Lin X, Yang L, Al-Abed Y, Wang H, Metz C, Miller EJ, Tracey KJ, Ulloa L, 2004 Cholinergic agonists inhibit HMGB1 release and improve survival in experimental sepsis. *Nat. Med* 10, 1216–1221. 10.1038/nm1124. [PubMed: 15502843]
- Westlund KN, Bowker RM, Ziegler MG, Coulter JD, 1981 Origins of spinal noradrenergic pathways demonstrated by retrograde transport of antibody to dopamine-beta-hydroxylase. *Neurosci. Lett* 25, 243–249. [PubMed: 6170028]
- Wright HL, Moots RJ, Edwards SW, 2014 The multifactorial role of neutrophils in rheumatoid arthritis. *Nat. Rev. Rheumatol* 10, 593–601. 10.1038/nrrheum.2014.80. [PubMed: 24914698]

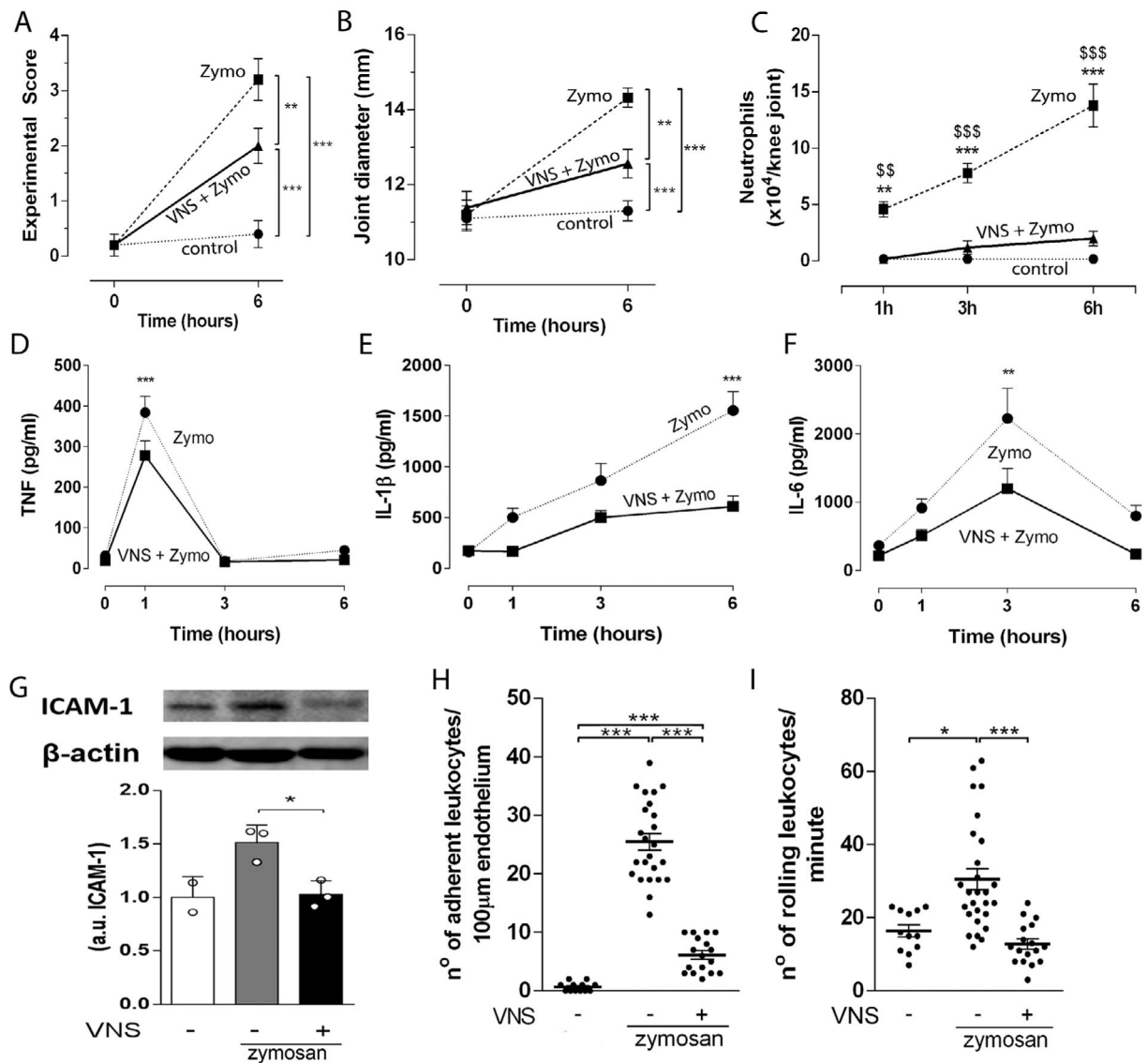


Fig. 1. VNS controls local inflammation via the sympathetic activity modulation. VNS improved knee (A) experimental score, (B) articular edema, (C) neutrophil count ($n = 5$ for each group), and synovial levels of (D) TNF, (E) IL-1 β , and (F) IL-6 at 0, 1, 3 and 6 h (0 h, $n = 2$; 1 h, $n = 4$; 3 h, $n = 3$; 6 h, $n = 4$) after intra-articular zymosan. Data were analyzed using two-way ANOVA followed by a Bonferroni's multiple comparison test comparing individual time-point. (G) Synovial ICAM-1 expression observed 6 h after vagal stimulation. Number of adherent (H) and rolling (I) leukocytes observed 1 h after VNS in the synovial endothelium in zymosan-injected knee-joints. Data were analyzed using one-way ANOVA followed by Tukey's multiple comparison test. $**p < 0.01$; $***p < 0.001$ versus control, $$$p < 0.01$; $$$$p < 0.001$ versus VNS + Zymo.

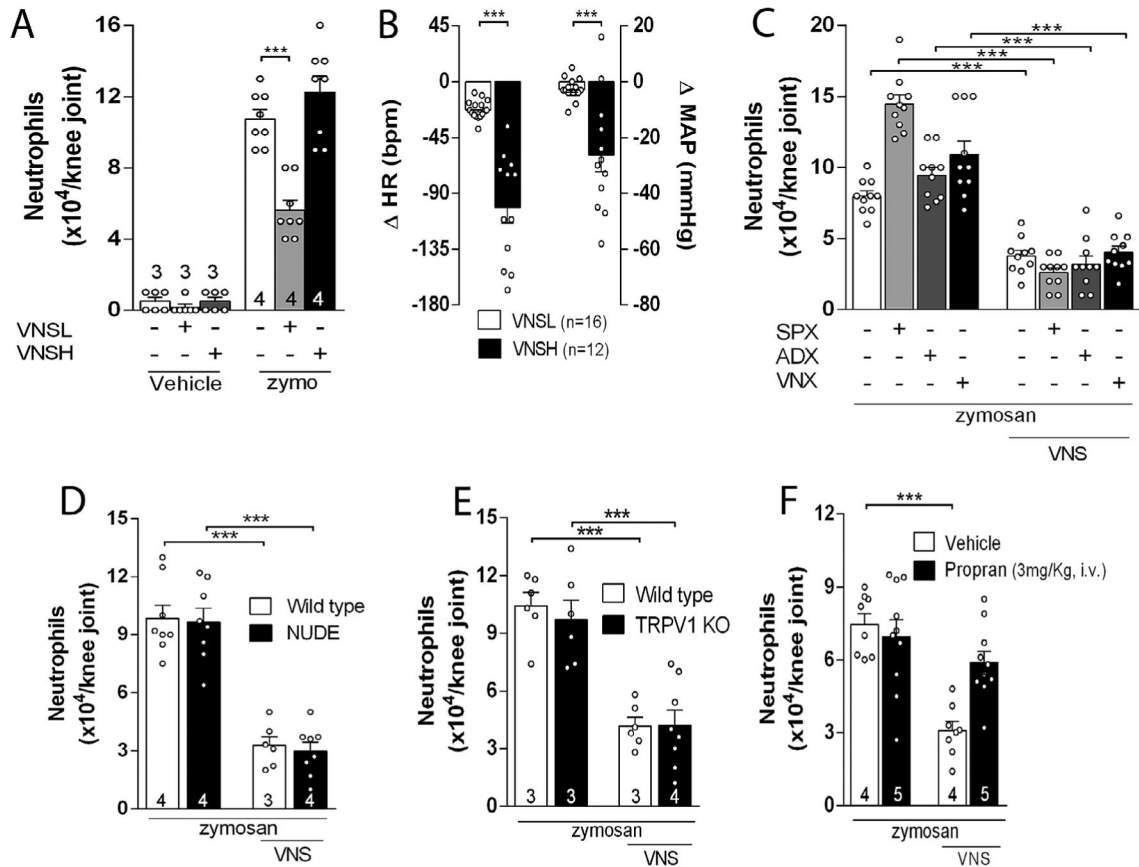


Fig. 2.

Low intensity VNS reduces articular inflammation by a new neuroimmune pathway. (A) Effects of VNS of high (VNSH: 5 Hz, 0.1 ms, 3 V) or low (VNSL: 5 Hz, 0.1 ms, 1 V) intensity on neutrophil migration and on (B) heart rate (HR) and mean arterial pressure (MAP); The anti-inflammatory effect of VNS is maintained after (C) splenectomy (SPX), adrenalectomy (ADX), or subdiaphragmatic vagotomy (sVNX) ($n = 5$ for each group), and in (D) NUDE or (E) TRPV1 KO mice, but not in (F) propranolol (Propan) treated-animals. Data were analyzed using one-way ANOVA followed by Tukey's multiple comparison test; The number of animals used for each group is displayed at the bottom of the corresponding bar. *** $p < 0.001$ versus control.

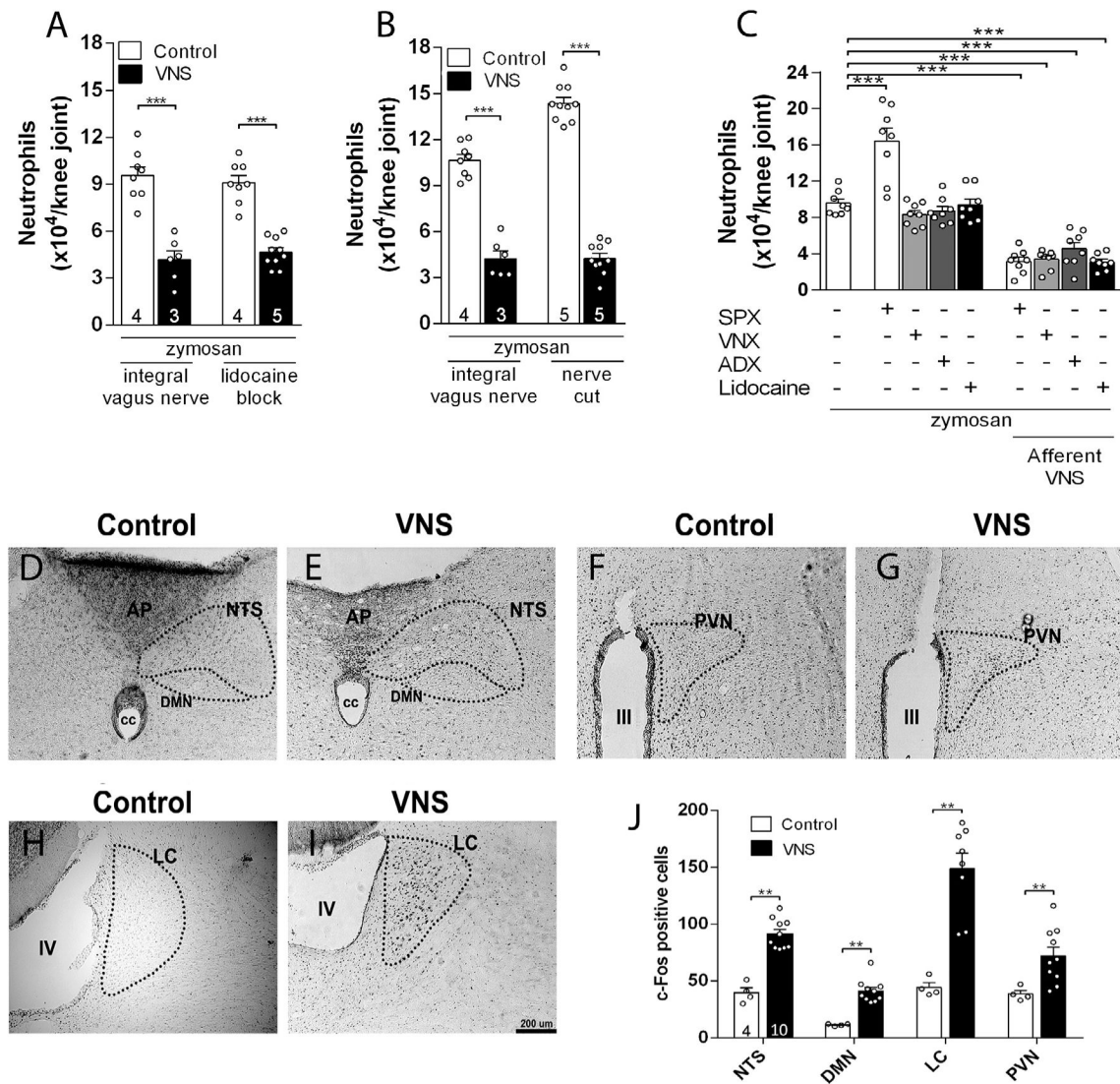


Fig. 3. Afferent VNS reduces articular inflammation and activates brain structures. Afferent VNS via (A) intra-nerve administration of lidocaine or (B) via surgical cut reduces knee inflammation. Afferent vagal stimulation reduces peripheral inflammation in (C) splenectomized (SPX), subdiaphragmatic vagotomized (sVNX) or adrenalectomized (ADX) rats ($n = 4$ for each group). Data were analyzed using one-way ANOVA followed by Tukey's multiple comparison test; VNS increases the expression of c-Fos in (D-E) the nucleus of the tractus solitarius (NTS), dorsal motor nucleus (DMN), (F-G) hypothalamic paraventricular nucleus (PVN), and (H-I) locus coeruleus (LC) as compared to the control (non-stimulated) group (D-J). Unpaired Student t -test was applied to this comparison. The number of animals used for each group is displayed at the bottom of the corresponding bar. $**p < 0.01$; $***p < 0.001$.

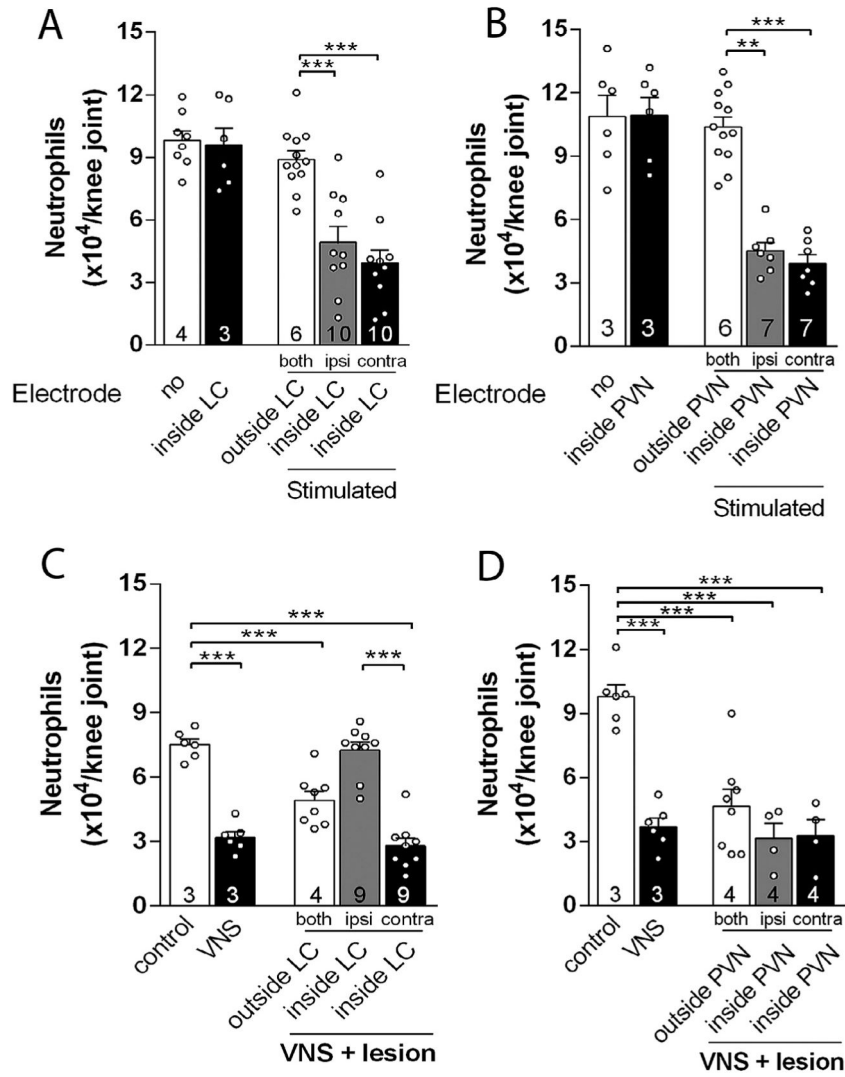


Fig. 4. Central structures activation is essential to the vagal anti-inflammatory effect. Electrical stimulation of the (A) LC or the (B) PVN decreases neutrophil migration into both knee joints. Temporary deactivation by prior injection of CoCl₂ into the (C) LC, but not (D) PVN, abrogated the vagal anti-inflammatory effect only in the ipsilateral, but not in the contralateral, joint to the hemispheric LC deactivation. Both: both knees; Ipsi: ipsilateral knee to the injected brain hemisphere; Contra: contralateral knee to the injected brain hemisphere. Data were analyzed using one-way ANOVA followed by Tukey’s multiple comparison test. The number of animals used for each group is displayed at the bottom of the corresponding bar. ***p* < 0.01; ****p* < 0.001.

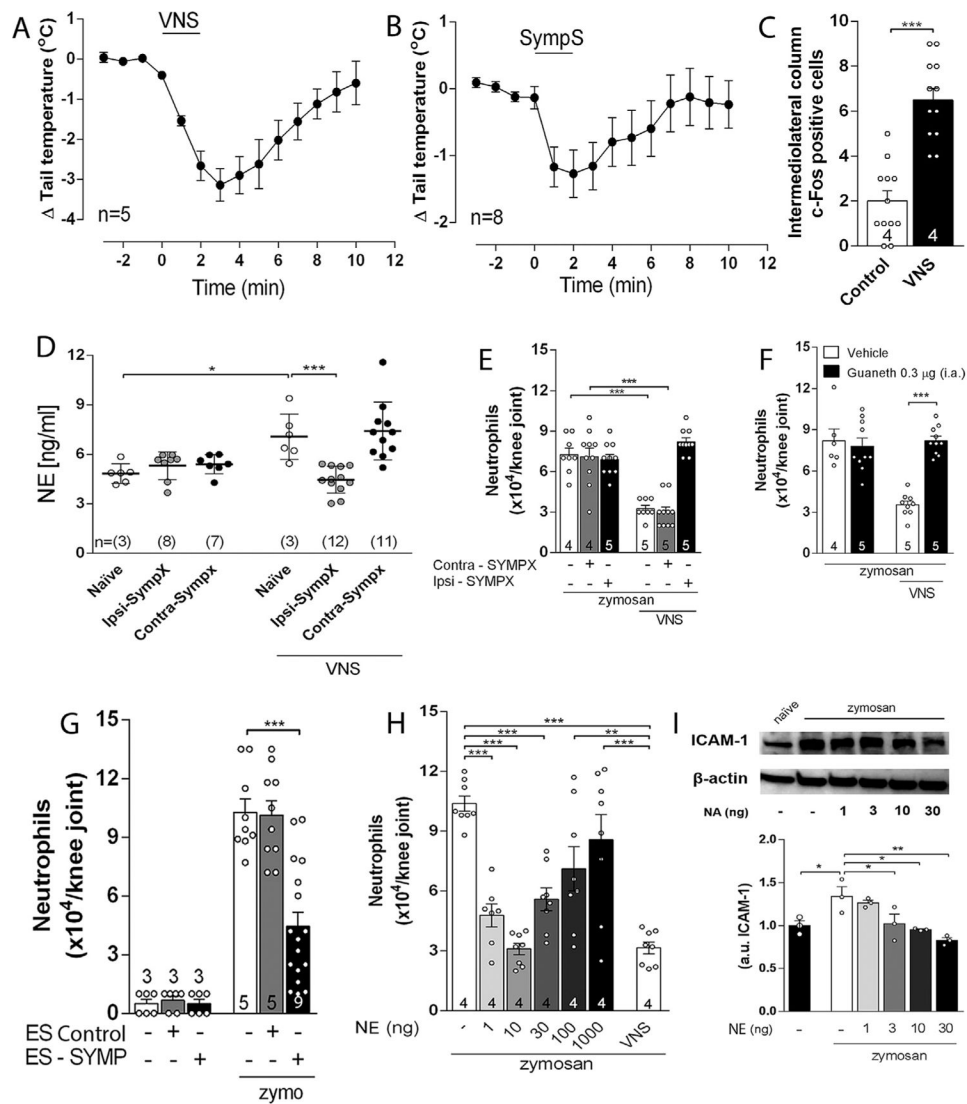


Fig. 5. Vagal anti-inflammatory signaling depends on local sympathetic system to evoke its anti-inflammatory effect. (A) Intact vagus nerve stimulation (VNS) or (B) sympathetic chain stimulation (SympS) decreases rat tail temperature; (C) VNS increases c-Fos expression in both sides of the intermediolateral column of the spinal cord; (D) Measurement of norepinephrine (NE) 5 min after VNS in the ipsilateral (Ipsi-SYMPX) and contralateral (Contra-SYMPX) joint to surgical sympathectomy (ELISA); (E) VNS anti-inflammatory effect is blocked in the ipsilateral (Ipsi-SYMPX), but not in the contralateral (Contra-SYMPX), joint by surgical sympathectomy; (F) VNS effect is blocked by prior intra-articular administration of guanethidine (Guaneth), the contralateral joint received vehicle solution; (G) Stimulation of the sympathetic chain (ES-SYMP), but not sham stimulation (ES Control), decreases neutrophil migration to the inflamed joints; (H-I) Intra-articular administration of NA decreases synovial ICAM-1 expression and neutrophil migration to the inflamed joint. Data were analyzed using one-way ANOVA followed by Tukey's multiple

comparison test. The number of animals used for each group is displayed at the bottom of the corresponding bar. * $p < 0.05$; ** $p < 0.01$; *** $p < 0.001$.

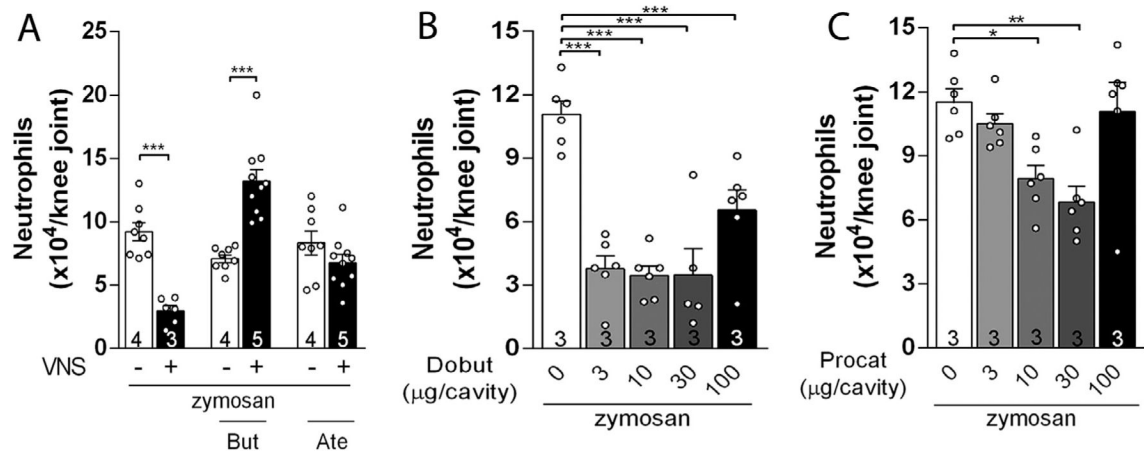


Fig. 6.

The activation of joint β -adrenergic receptors is mandatory for the central vagal anti-inflammatory signaling. Intra-articular administration of (A) β_2 (Butoxamine – But) or β_1 (Atenolol – Ate) antagonists abrogate the anti-inflammatory effects of VNS; Intra-articular injection of (B) β_1 (Dobutamine – Dobut) or (C) β_2 (Procaterol – Procat) agonists decrease knee inflammation. Data were analyzed using one-way ANOVA followed by Tukey's multiple comparison test. The number of animals used for each group is displayed at the bottom of the corresponding bar. * $p < 0.05$; ** $p < 0.01$; *** $p < 0.001$.

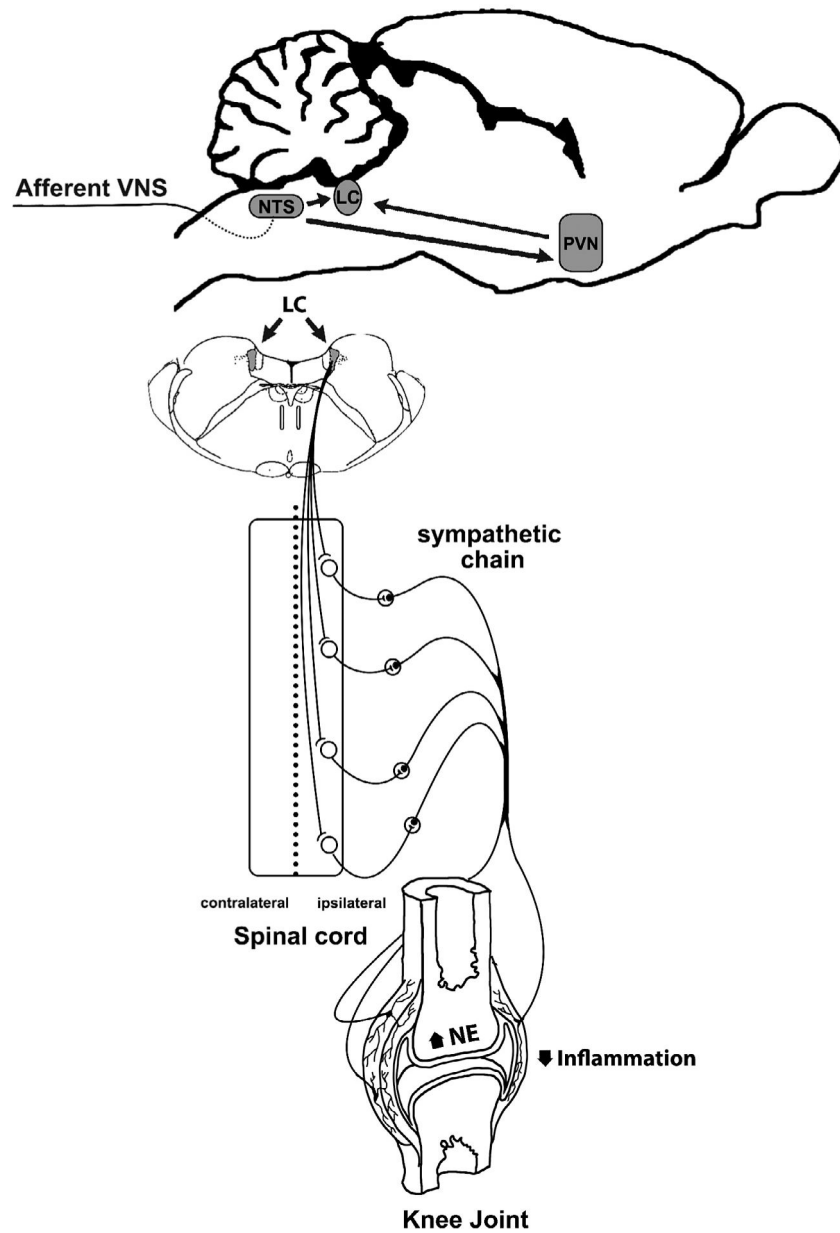


Fig. 7. Comprehensive illustration of the central inflammatory processing centers (LC and PVN) activated through afferent vagal stimulation. Afferent VNS (green) controls arthritic joint inflammation by activating specific sympho-excitatory brain areas (blue) and sympathetic nerve fibers to increase synovial norepinephrine (NE) levels to reduce articular inflammation. (For interpretation of the references to colour in this figure legend, the reader is referred to the web version of this article.)